IOP PUBLISHING EUROPEAN JOURNAL OF PHYSICS

Eur. J. Phys. **29** (2008) 385–392 doi:10.1088/0143-0807/29/2/018

Inverted spring pendulum driven by a periodic force: linear versus nonlinear analysis

A Arinstein[1,2] **and M Gitterman**[1]

[1] Department of Physics, Bar-Ilan University, Ramat-Gan 52900, Israel
[2] Department of Mechanical Engineering, Technion-Israel Institute of Technology, Haifa 32000, Israel

Received 2 December 2007, in final form 4 February 2008
Published 22 February 2008
Online at stacks.iop.org/EJP/29/385

Abstract

We analyse the stability of the spring inverted pendulum with the vertical oscillations of the suspension point. An important factor in the stability analysis is the interaction between radial and oscillating modes. In addition to the small oscillations near the upper position, the nonlinearity of the problem leads to the appearance of limit-cycle oscillations of finite amplitudes.

1. Introduction

A proven method of studying different phenomena in nature is the use of simplified models. While the harmonic oscillator is the simplest linear model, most if not all of these phenomena are nonlinear, and one of the simplest models for their description is a pendulum, consisting of a bob of mass m suspended on a rod of length l and able to perform oscillations about the vertical position. A tremendous amount of effort has been devoted to the study of the pendulum [1].

A simple pendulum has two equilibrium positions which we call down or up. Obviously the down position is stable, and the up position is unstable. Stability means that, being displaced from its initial position the pendulum, after a few transient oscillations, returns to this position due to friction. Next in order of complexity is a spring (or elastic, or extensible) pendulum which is defined as a simple pendulum with a spring of a stiffness constant κ, inserted in its rod. When the spring frequency $\omega_s^2 = \kappa/m$ is about twice the pendulum frequency $\hat{\omega}_0^2 = g/l$, a spring pendulum performs periodic oscillations about its upper position [2]. Another possibility exists of transforming the unstable upward position of a simple pendulum into a stable one, namely one can add vertical oscillations $u = A\cos(\Omega t)$ of the suspension point. This phenomenon of the so-called parametric resonance was predicted by Stephenson in as early as 1908 [3]. The upward position of a simple pendulum becomes stable when the condition $A^2\Omega^2 > 2gl$ is satisfied [4].

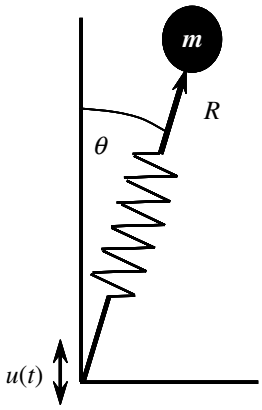

Figure 1. System of coordinates used in the text.

Both in a spring pendulum and in a periodically driven pendulum, the stabilization of the upper position is defined by some relation between two characteristic frequencies, ω_s and $\hat{\omega}_0$ in the first case, and $\hat{\omega}_0$ and Ω in the second one. The aim of this paper is the integration of these two cases in an effort to find the relation between three characteristic frequencies, $\hat{\omega}_0$, ω_s and Ω which allow the stabilization of the inverted spring pendulum driven by a periodic force. Previous workers [5, 6] considered a similar problem, but they restricted themselves to the stability analysis in a linear approximation using the linear Floquet theory [5], or to an external field of small amplitude using the method of multiple scales [6]. In contrast to these articles, we perform the full nonlinear analysis of stability. Some new effects are to be expected, such as the resonance between the spring frequency ω_s and the external frequency Ω. Note that for finite amplitudes, the motion of the system permits chaos which is excluded from our analysis. The inverted pendulum is an important part of modern control devices.

2. Dynamic equations

The position of the bob m moving in a vertical plane can be characterized by the polar coordinates R and θ (figure 1), where $R(t)$ is the pendulum length at time t ($R \equiv l$). For a spring pendulum without the external oscillations the Lagrangian is [7]

$$L_0 = \frac{m}{2}\left[\left(\frac{\mathrm{d}R}{\mathrm{d}t}\right)^2 + \left(R\frac{\mathrm{d}\theta}{\mathrm{d}t}\right)^2\right] - mgR\cos\theta - \frac{\kappa}{2}(R - l_0)^2. \tag{1}$$

An additional oscillation of the suspension point $u(t) = A\cos(\Omega t)$ is taken into account as follows. The suspension point has acceleration $\mathrm{d}^2u/\mathrm{d}t^2$ relative to the inertial frames of reference. We introduce a non-inertial frame which itself has this acceleration. In this frame, the gravity constant g is replaced by $g + \mathrm{d}^2u/\mathrm{d}t^2$, so

$$L = \frac{m}{2}\left[\left(\frac{\mathrm{d}R}{\mathrm{d}t}\right)^2 + \left(R\frac{\mathrm{d}\theta}{\mathrm{d}t}\right)^2\right] - m\left(g + \frac{\mathrm{d}^2u}{\mathrm{d}t^2}\right)R\cos\theta - \frac{\kappa}{2}(R - l_0)^2. \tag{2}$$

The equations of motion can be easily obtained from the Lagrangian (2). When the bob starts to oscillate near the downward position, one obtains the following equations of motion

for $\hat{\theta} = \pi - \theta$ and r,

$$\frac{\mathrm{d}^2 r}{\mathrm{d}t^2} + \omega_s^2 r = \left(1 - \frac{\omega_0^2}{\omega_s^2} + r\right)\left(\frac{\mathrm{d}\theta}{\mathrm{d}t}\right)^2 + \omega_0^2(1 - \cos\theta) - \frac{1}{l_0}\frac{\mathrm{d}^2 u}{\mathrm{d}t^2}\cos\theta, \tag{3}$$

$$\frac{\mathrm{d}^2\theta}{\mathrm{d}t^2} + \frac{2}{1 - \omega_0^2/\omega_s^2 + r}\frac{\mathrm{d}r}{\mathrm{d}t}\frac{\mathrm{d}\theta}{\mathrm{d}t} - \frac{1}{1 - \omega_0^2/\omega_s^2 + r}\left(\omega_0^2 + \frac{1}{l_0}\frac{\mathrm{d}^2 u}{\mathrm{d}t^2}\right)\sin\theta = 0, \tag{4}$$

where the dimensionless relative elongation r of the pendulum is defined as

$$r = \frac{R}{l_0} - \left(1 + \frac{\omega_0^2}{\omega_s^2}\right). \tag{5}$$

When $u(t) \equiv 0$, equations (3) and (4) are transformed into well-known equations for the spring pendulum [7, 8]. The equations of motion near the downward position differ from equations (3) and (4) in the signs of ω_0^2 and $u(t)$.

Note that the oscillator frequency ω_0^2 is defined relative to the constant parameter l_0, $\omega_0^2 = g/l_0$, in contrast to the frequency $\hat{\omega}_0^2$ defined with respect to the variable length l, $\hat{\omega}_0^2 = g/l$, as is done usually. In such a way we keep the frequencies ω_0 and ω_s independent of one another.

The linearized equations (3) and (4) with $u(t) = A\cos(\Omega t)$, written in terms of a dimensionless time $\tau = \Omega t$, have the following form

$$\frac{\mathrm{d}^2 r}{\mathrm{d}\tau^2} + \frac{\omega_s^2}{\Omega^2} r = A\cos(\tau), \tag{6}$$

$$\frac{\mathrm{d}^2\theta}{\mathrm{d}\tau^2} - \frac{1}{1 - \omega_0^2/\omega_s^2}\left[\frac{\omega_0^2}{\Omega^2} - \frac{A}{l_0}\cos(\tau)\right]\theta = 0. \tag{7}$$

Equation (6) is the equation of a driven harmonic oscillator while (7) is the Mathieu equation. There exists a comprehensive literature about Mathieu equations of the general form

$$\frac{\mathrm{d}^2\theta}{\mathrm{d}t^2} + [\alpha + \beta\cos(t)]\,\theta = 0, \tag{8}$$

where for the oscillations about the downward position the stable regions alternate with the unstable ones. For the oscillations about the upper position the single stable region, bounded by the dashed lines, is shown in figure 2.

It turns out [9, 10] that for a small amplitude β of an external field, the first zone of stability is bounded from below by the curve

$$\alpha = -0.5\beta^2. \tag{9}$$

In terms of our parameters (7), this curve is

$$\frac{\omega_0^2}{\Omega^2} = \frac{0.5}{1 - \omega_0^2/\omega_s^2}\left(\frac{A}{l_0}\right)^2. \tag{10}$$

For the upper border of the stability region, one has [9, 10]

$$\alpha = 0.25 - 0.556\beta, \tag{11}$$

which in terms of our parameters, is

$$\frac{\omega_0^2}{\Omega^2} = 0.556\left(\frac{A}{l_0}\right) - 0.25\left(1 - \frac{\omega_0^2}{\omega_s^2}\right). \tag{12}$$

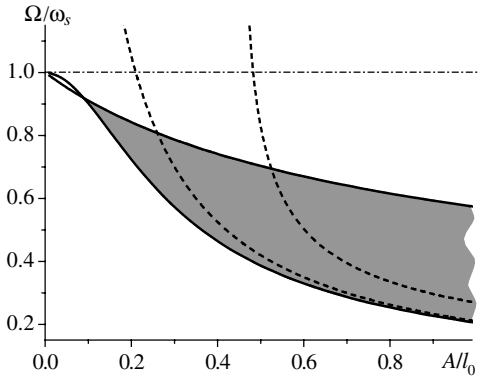

Figure 2. The stability–unstability phase diagram in $(\Omega/\omega_s;\, A/l_0)$ dimensionless variables for constant $\omega_0/\omega_s = 0.1$. The dashed lines, which confine the stable region, are found from the linear analysis of the Mathieu equation. The shadowed region, restricted by two solid lines, defines the stability region obtained by numerical solution of the nonlinear equations.

In addition to the two stable points $\theta = \pi$ and $\theta = 0$, equations (3) and (4) may show instabilities with respect to θ (strong oscillations or rotations of the pendulum) and with respect to r for some values of the parameters. During the oscillations of a spring pendulum the elastic energy of a spring switches back and forth to the mechanical energy of oscillations. This energy exchange between these two modes is similar to the transition between kinetic and potential energies in a simple pendulum where the energy switches back and forth between the potential energy, which is maximal at two highest positions of a bob, and the kinetic energy which is maximal in the vertical orientations. The energy exchange between oscillating and elastic modes may result in a large elongation of the spring, which is even able to exceed the margin of safety of a spring and to tear it. The analysis of these phenomena requires the full solution of the nonlinear equations (3) and (4).

Due to oscillations of the suspension point, the upward position becomes stable if the following condition is fulfilled [4],

$$A^2\Omega^2 > 2gl \equiv 2\omega_0^2 l_0 l. \tag{13}$$

In the upward position, due to the elastic force and gravity, the length l of a spring pendulum decreases from its initial length l_0 to $l = l_0 - mg/\kappa = l_0\left(1 - \omega_0^2/\omega_s^2\right)$. Substituting the latter formula into (13), one can rewrite the boundary of stability of the upward position of the pendulum in the following form,

$$\frac{\Omega}{\omega_s} = \frac{\omega_0}{\omega_s}\sqrt{2\left(1 - \omega_0^2/\omega_s^2\right)} \cdot \frac{l_0}{A}. \tag{14}$$

The second boundary of stability of the upward position of the pendulum (12) can be rewritten in a similar form

$$\frac{\Omega}{\omega_s} = \frac{\omega_0/\omega_s}{\sqrt{0.556(A/l_0) - 0.25\left(1 - \omega_0^2/\omega_s^2\right)}}. \tag{15}$$

Clearly, the amplitude of external oscillations A cannot be larger than the length l of the pendulum, $A < l$.

In addition to the transition from (13) to (14), the presence of a spring results in new effects. We shall discuss two such effects which have not yet been sufficiently explored.

(1) If the characteristic frequency of the driving force Ω is of the order of the characteristic frequency of the spring, ω_s, the resonance phenomenon of radial motion takes place (especially for small θ), and the pendulum becomes unstable. In spite of the fact that the frequency of the spring is incorporated into equations (14) and (15), which describe the stability–instability curves, the impact of the resonance phenomenon on these stability–instability curves is much more important. Indeed, according to a linear analysis of the Mathieu-type equation, these two curves, (14) and (15), cross the $\Omega - \omega_s$ resonance curve, upon which the system becomes unstable. Hence, we expect that a nonlinear analysis will produce stability–instability curves that are substantially different from the linear results (14) and (15).

(2) A comparison of equations (3) and (6) shows that in the linear approximation, the time dependence of $r(t)$ is determined by the external field, and the influence of the angular mode for small θ is described by the $r(\mathrm{d}\theta/\mathrm{d}t)^2$ term. The latter means that for small $\theta(t=0)$, say, equal to 10^{-4}, the appropriate $r(t)$ may not be small. On the other hand, an external field enters equation (7) multiplicatively, thereby exerting much weaker control over $\theta(t)$ than over $r(t)$. The solution of the inhomogeneous linearized equation (6) has the following form

$$r = \frac{\Omega^2}{\omega_s^2 - \Omega^2} \cdot \frac{A}{l_0} \cos\tau = \frac{(\Omega/\omega_s)^2}{1 - (\Omega/\omega_s)^2} \cdot \frac{A}{l_0} \cos\tau, \tag{16}$$

and an increase of the amplitude of $r(t)$ which may produce an instability in θ, occurring either by increasing A at constant Ω/ω_s, or by increasing Ω/ω_s at constant A.

Hence, we conclude that the above linear analysis of stability does not exhaust the stability analysis, and the numerical solution of the full nonlinear equations has to be performed.

3. Nonlinear analysis

The necessary numerical analysis was performed on the basis of the MathCad program with the help of the built-in function 'differential equations solver'. The results of the numerical analysis for constant $\omega_0/\omega_s = 0.1$, which are displayed in the $\{\Omega/\omega_s, A/l_0\}$ plane in figure 2, show the difference of the lower and upper stability–instability lines for the rigid pendulum (the dashed lines) and for the spring pendulum (the solid lines). When the lower stability–instability line for the rigid pendulum which, according to equation (14), has the form of a hyperbola $\Omega \approx A^{-1}$ approaches the resonance line $\Omega/\omega_s = 1$, the pendulum loses its stability. Thus, for a spring pendulum, the hyperbola $\Omega \approx A^{-1}$ does not go to infinity, as was the case for a rigid pendulum ($\omega_s = \infty$), but, rather, approaches the line $\Omega = \omega_s$. In this transition region, the boundary of stability (14) can be replaced by the empirical formula

$$\frac{\Omega}{\omega_s} = \frac{\omega_0/\omega_s \sqrt{2\left(1 - \omega_0^2/\omega_s^2\right)}}{\sqrt{2\omega_0^2/\omega_s^2\left(1 - \omega_0^2/\omega_s^2\right) + A^2/l_0^2}}, \tag{17}$$

which reduces to (14) for small Ω/ω_s, and describes the resonance $\Omega \simeq \omega_s$ for small A.

The upper stability–instability line for the rigid pendulum which is described by equation (15), intersects the resonance line $\Omega/\omega_s = 1$, and in the case of the spring pendulum, this line has to be modified. Instability of the oscillating mode comes from the increase of the amplitude of $r(t)$ (as was mentioned after equation (16)) which influences the amplitude $\theta(t)$ and results in instability. Therefore, we tried to describe the upper curve by the criterion

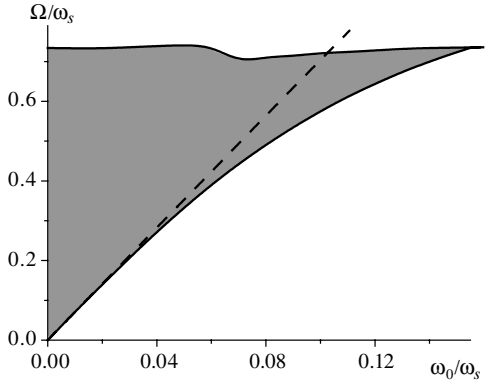

Figure 3. The stability–unstability phase diagram in $\{\Omega/\omega_s, \omega_0/\omega_s\}$ dimensionless variables for constant $A/l_0 = 0.2$. The dashed line which describes the lower instability–stability boundary, is found from the linear analysis of the Mathieu equation. The shadowed region, restricted by two solid lines, defines the stability region obtained by numerical solution of the nonlinear equations.

which follows from equation (16), namely, the instability occurs when the amplitude of $r(t)$ is sufficiently large:

$$\frac{(\Omega/\omega_s)^2}{1-(\Omega/\omega_s)^2} \cdot \left(\frac{A}{l_0}\right) \geqslant \hat{a}, \tag{18}$$

and the equation for the upper stability–instability curve has the following form

$$\frac{\Omega}{\omega_s} = \sqrt{\frac{\hat{a}}{\hat{a} + A/l_0}}, \tag{19}$$

where the parameter $\hat{a}$ depends on the initial conditions of the system. The dependence on the initial conditions follows from the fact that the solution of equation (6) consists of the sum of a partial solution of the inhomogeneous and the general solution of the homogeneous equation, whereas the amplitude of the latter depends on the initial conditions. In order to exclude the solution of the homogeneous equation, and, thereby exclude the influence of initial conditions on the value of parameter $\hat{a}$, we used in our numerical calculation the following initial conditions for the function $r(t = 0)$: $r(t = 0) = \frac{(\Omega/\omega_s)^2}{1-(\Omega/\omega_s)^2} A/l_0$ and $\dot{r}(t = 0) = 0$ which corresponds to the pure driven oscillations. In this case we found $\hat{a} \approx 0.5$.

The stability–instability phase diagram in the $(\Omega/\omega_s, \omega_0/\omega_s)$ plane is shown in figure 3, where the dashed line is derived from the linear analysis of the Mathieu equation while the solid lines were obtained from the numerical solutions of nonlinear equations.

At the end of the previous section we mentioned the two possible results of the numerical solution of the nonlinear equations which can be predicted on the basis of the linear analysis. It turns out, however, that the numerical solutions of the full nonlinear equations (3) and (4) show some peculiar features which cannot be found or predicted by linear analysis. The latter gives lower and upper lines bounding the stability region while the former shows some 'fine structure' of stable solutions. For small and fixed A/l_0, say, $A/l_0 = 0.2$, by increasing Ω/ω_s, one obtains only unstable solutions for $\Omega/\omega_s < 0.582$. At $\Omega/\omega_s = 0.582$, one crosses the lower stable–unstable line passing to stable solutions, and finally, for $\Omega/\omega_s = 0.848$ one returns to an unstable region. However, there are different types of stable solutions in the region $0.582 < \Omega/\omega_s < 0.848$. For initial displacement $\theta_0 = 10^{-4}$, the oscillations have amplitudes of the same order of magnitude for $0.582 < \Omega/\omega_s < 0.846$ (see figure 4 for $\Omega/\omega_s = 0.846$),

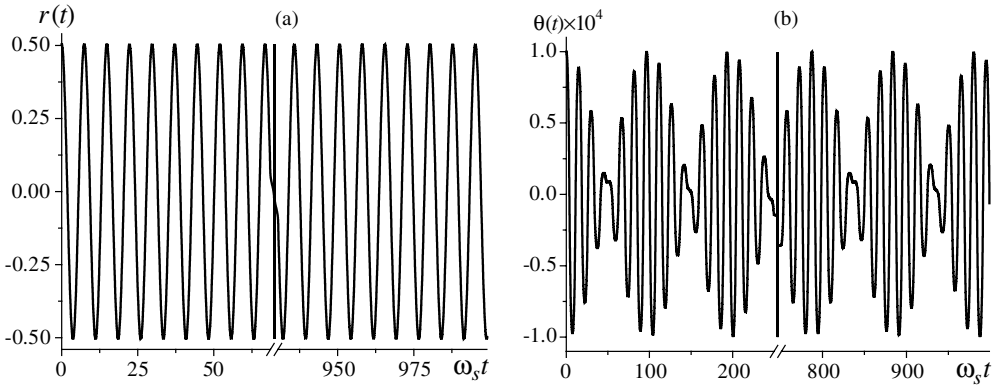

Figure 4. The time dependence of the radial, $r(t)$, and angle, $\theta(t)$, coordinates for $\Omega/\omega_0 = 0.846$, showing the small oscillations of $\theta(t)$.

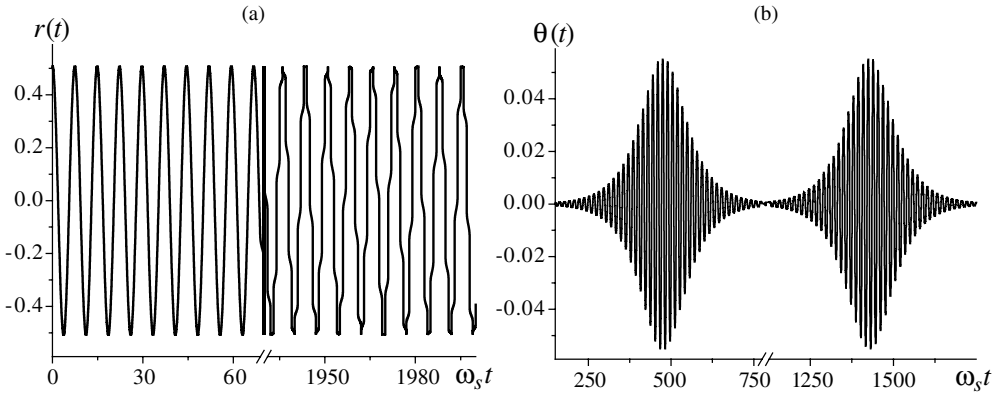

Figure 5. The same as in figure 3, but for $\Omega/\omega_0 = 0.847$, showing the large oscillations of $\theta(t)$.

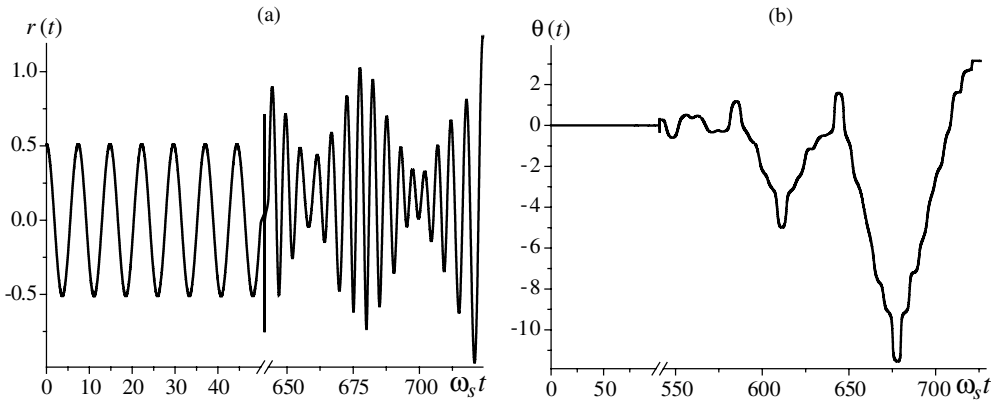

Figure 6. The same as in figure 3, but for $\Omega/\omega_0 = 0.848$, showing the instability of the pendulum.

whereas for $0.846 < \Omega/\omega_s < 0.848$ the same initial condition leads to limit-cycle oscillations of finite amplitudes (see figure 5 for $\Omega/\omega_s = 0.847$). And finally, as was mentioned above, for $\Omega/\omega_s \geqslant 0.848$ the instability in $\theta(t)$ occurs (see figure 6 for $\Omega/\omega_s = 0.848$). In figures 4–6 we show also the amplitude $r(t)$ of radial oscillations, which remains finite for all these cases, and reaches the value of $r(t) \approx 1$ for the instability case.

For larger values of A/l_0, or for different initial conditions this phenomenon—alternation of small oscillations and limit cycles—occurs many times in the stable region of the parameters. Note that such multiple-nodding oscillations have been found for a rigid pendulum [11].

4. Conclusion

We have considered the elastic pendulum subject to rapid vertical oscillations of the suspension point. The stability conditions of such a pendulum are defined by the relationship between the amplitude of an external field A and the frequencies ω_0 of a pendulum, ω_s of a spring, and Ω of a field. This analysis is a generalization of the well-known cases of a spring pendulum ($A = 0$) and an inverted pendulum ($\omega_s = \infty$). The analytic solution of the linear problem and numerical simulations of nonlinear equations yield some new results, such as the influence of resonance between the frequency of a spring and that of an external force on the stability conditions, instability for small initial disturbances which occurs due to the mode coupling, and the appearance of limit-cycle oscillations near the upper position of the pendulum.

We hope that our treatment may be appropriate as an integral part of an undergraduate course in classical mechanics. Moreover, let us mention some problems connected with this paper, which can be proposed as projects which are appropriate for students:

(1) Find the influence of a damping force on the stability diagrams by adding a damping term proportional to the first derivatives into equations (3) and (4), and performing the numerical calculations. Pay special attention to the shift of stability–instability lines, stability of the upward position and existence of limit cycles.
(2) For small angles θ one can replace sin θ and cos θ by their power series. Perform the appropriate calculations for the linear equation, and compare the results obtained with those following from the nonlinear analysis.
(3) As was shown by Miles [12] the upward position is stable when the dynamic equation of the rigid pendulum contains an additional time-periodic term. Analogously to the present work, consider the stability diagram when the rigid pendulum is replaced by the spring one.

References

[1] Gauld C 2004 *Sci. Educ.* **13** 811
[2] Vitt A A and Gorelik G S 1933 *Zh. Tekh. Fiz. Sovietunion* **3** 291 (in Russian)
[3] Stephenson A 1908 *Mem. Proc. Manch. Lit. Phil. Soc.* **52** 1
[4] Landau L and Lifschitz E 1956 *Mechanics* (Oxford: Pergamon)
[5] Ryland G and Meirovitch L 1977 *J. Sound Vibr.* **51** 547
[6] Mazzilli C E N 1985 *IMA J. Appl. Math.* **34** 137
[7] Lynch P 2002 *Int. J. Non-Lin. Mech.* **37** 345
[8] Phelps F M and Hunter J H 1965 *Am. J. Phys.* **33** 285
[9] McLachlan N W 1947 *Theory and Applications of Mathieu Functions* (Oxford: Clarendon)
[10] Blackburn J A, Smith H J T and Gronbech-Jensen N 1992 *Am. J. Phys.* **60** 907
[11] Acheson D J 1995 *Proc. R. Soc.* A **448** 89
[12] Miles J 1998 *Phys. Lett.* A **133** 295